1 JHG-18-688 R2

2 ARTICLE

3 **Identification of a homozygous frameshift variant in *RFLNA* in a**

4 **patient with a typical phenotype of spondylocarpotarsal synostosis**

5 **syndrome**

6

7 **Hitomi Shimizu[1,2], Satoshi Watanabe[1,] Akira Kinoshita[2], Hiroyuki Mishima[2], Gen**

8 **Nishimura[3], Hiroyuki Moriuchi[1], Koh-ichiro Yoshiura[2], and Sumito Dateki[1*]**

9

10 [1] Department of Pediatrics, Nagasaki University Graduate School of Biomedical

11 Sciences, Nagasaki, Japan

12 [2] Department of Human Genetics, Nagasaki University Graduate School of Biomedical

13 Sciences, Nagasaki, Japan

14 [3] Center for Intractable Disease, Saitama Medical University Hospital, Saitama, Japan

15

16 **Running title:** A patient with a homozygous *RFLNA* mutation

17

18 **Conflicts of interest:** The authors declare no conflicts of interest in association with the

19 present study.

23

24 *Correspondence to

25 Sumito Dateki, M.D.

26 Department of Pediatrics, Nagasaki University Graduate School of Biomedical Sciences

27 Address: 1-7-1 Sakamoto, Nagasaki, 852-8501 Japan

28 E-mail: sdateki1@nagasaki-u.ac.jp

29 Phone: +81-95-819-7298, FAX: +81-95-819-7301

30

Abstract

Spondylocarpotarsal synostosis syndrome, a rare syndromic skeletal disorder

characterized by disrupted vertebral segmentation with vertebral fusion, scoliosis, short

stature and carpal/tarsal synostosis, has been associated with biallelic truncating

mutations in the filamin B gene or monoallelic mutations in the myosin heavy chain 3

gene. We herein report the case of a patient with a typical phenotype of

spondylocarpotarsal synostosis syndrome who had a homozygous frameshift mutation

in the refilin A gene (*RFLNA)* [c.241delC, p.(Leu81Cysfs*111)], which encodes one of

the filamin binding proteins. Refilins, filamins, and myosins play critical roles in

forming perinuclear actin caps, which change the nuclear morphology during cell

migration and differentiation. The present study implies that *RFLNA* is an additional

causative gene for spondylocarpotarsal synostosis syndrome in humans and a defect in

forming actin bundles and perinuclear actin caps may be a critical mechanism for the

development of spondylocarpotarsal synostosis syndrome.

45

Introduction

Spondylocarpotarsal synostosis syndrome (SCT) (OMIM #272460) is characterized by disrupted vertebral segmentation with vertebral fusion, scoliosis, short stature, and carpal/tarsal synostosis. Mutations in filamin B (*FLNB*) (NM_001457) and myosin heavy chain 3 (*MYH3*) (NM_002470) have been identified in patients with autosomal recessive and autosomal dominant SCT, respectively [1-3].

Mutations in *FLNB* cause five distinct skeletal diseases (SCT, Larsen syndrome, atelosteogenesis type I, atelosteogenesis type III, and boomerang dysplasia). Among these, only SCT is inherited in an autosomal recessive manner; the others are inherited in an autosomal dominant manner [4]. *FLNB* mutations have been reported in at least 16 families with SCT [5], all of whom showed either nonsense or frameshift biallelic mutations predicted to induce premature translation termination or consecutive changes in amino acid sequences, indicating that conditions brought about by severe FLNB defects are associated with phenotypes of SCT [1, 2, 4].

Filamins are dimeric actin binding proteins [6]. Refilin A (RFLNA) and Refilin B (RFLNB) (also known as FAM101A and FAM101B, respectively) have been identified as vertebrate-specific short-lived filamin-binding proteins. Under TGF-β stimulation, filamins bind to RFLNs and transform their connecting actins into parallel bundle structures that accumulate each other to form perinuclear actin caps (Fig. 1a, b, c). A series of the processes above is important for cell migration and differentiation leading to endochondral ossification and skeletal development [6, 7].

We herein report the case of a Japanese boy with a typical phenotype of SCT who had a homozygous frameshift variant in *RFLNA* (NM_181709). We propose that *RFLNA* is an additional causative gene for SCT in humans.

70 **Materials and methods**

71 **Case report**

72   The patient was born at 34 weeks of gestation. At birth, his length was 43 cm (-0.7 SD)

73 and his weight was 2.35 kg (+0.3 SD). An X-ray examination at the time of birth

74 showed seemingly normal segmented vertebrae. At 1 year and 2 months of age, the

75 patient was referred to us because of severe short stature. His height was 67.2 cm (-3.7

76 SD), weight 7.8 kg (-2.2 SD), and occipital frontal circumference 47 cm (+1.1 SD). He

77 also had mild facial dysmorphic features with frontal bossing and anteverted nares. A

78 skeletal survey showed spondylar fusion mainly affecting the posterior neural arches

79 and to a lesser degree the vertebral bodies with mild scoliosis and carpo-tarsal

80 synostosis (fusion of the capitate and hamate and probably that of the cuboid and lateral

81 cuneiform) (Fig. 2). He was diagnosed with SCT based on his characteristic skeletal

82 features, severe short stature, and progressive clinical course. At the last examination at

83 2 years and 3 months of age, he was 72.4 cm tall (-4.3SD). His motor and mental

84 development was normal. The patient's parents were non-consanguineous. The patient's

85 father and elder brother were phenotypically normal, while his mother showed short

86 stature (147 cm, –2.2 SD) without dysmorphic facial features or scoliosis.

87 **Whole exome sequencing**

88 The family underwent trio whole-exome sequencing (WES). Genomic DNA extracted

89 from peripheral blood leukocytes was captured using Agilent SureSelect Exome Target

90 Enrichment System v6 (Agilent Technologies, Santa Clara, CA, USA) and sequenced

91 on a HiSeq^{TM} 2500 (Illumina, San Diego, CA, USA) with 150 bp paired-end reads.

92 Fastq format files were generated and aligned on the hg19/GRCh37 human reference

93 genome sequence using the Novoalign software program (Novocraft Technologies,

94   Kuala Lumpur, Malaysia). The Genome Analysis Toolkit (GAKT HaplotypeCaller) was

95   used for variant calling and consequently implemented in an in-house workflow

96   management tool [8,9]. Single nucleotide variations and insertions/deletions were

97   annotated using the ANNOVAR software program [10]. Then, rare and deleterious

98   variants were filtered using a previously described method [11]. Based on this pedigree,

99   autosomal dominant, recessive, and X-linked recessive models of inheritance were

100   assumed for the analysis. This study was approved by the Institutional Review Board

101   Committee at Nagasaki University Graduate School of Biomedical Sciences.

102   **PCR-based expression analyses of *RFLNA***

103   Total RNA was extracted from lymphoblastoid cell lines derived from the proband with

104   the *RFLNA* mutation and the parents using the NucleoSpin RNA Plus kit (Takara,

105   Shiga, Japan). RNA (2.0 μg) was reverse transcribed using the PrimeScript™ II 1st

106   strand cDNA Synthesis Kit (Takara). The obtained cDNA and control genome DNA

107   were amplified by PCR with primers for exon 2 (5'-GCATCAAGGTGAACCCGGA-

108   3') and the 3' untranslated region in exon 3 (5'- GGCTGTTCTCTGCTTCAAGG-3')

109   for the *RFLNA* gene, as well as those for exon 5 (5'-

110   GAACAAGGTTAAAGCCGAGCC-3) and exon 6 (5'-

111   GTGGCAGATTGACTCCTACCA-3') for the *PGK1* gene (NM_000291), which was

112   utilized as an internal control. Subsequently, the PCR products were subjected to direct

113   sequencing.

114

115   **Results**

116   Trio WES revealed a homozygous frameshift variant in the last exon 3 of the *RFLNA*

117   gene in the patient (chr12:124 798 904C>- [GRCh37/hg19]; c.241delC [NM_181709])

118   (Fig. 3a). The parents were heterozygous for the variant. The mutational analyses were

119   not done for the phenotypically normal elder brother. This variant is predicted to cause a

120   frameshift at codon 81 for *RFLNA*, skip the initial 136th termination codon, and result in

121   the production of an additional 110 aberrant amino acids (p.(Leu81Cysfs*111))

122   (NP_859060). PCR-based expression and sequence analyses using cDNA derived from

123   lymphoblastoid cell lines showed that the mutant allele was expressed in the patient

124   (Fig. 3b), and the mutant and the wild type alleles were expressed in the parents with

125   the heterozygous *RFLNA* variant (data not shown; Fig. 3b) [6]. The variant in *RFLNA*

126   has not been registered in the following databases: 1000G (www.1000genomes.org),

127   Exome Aggregation Consortium (ExAC; http://exac.broadinstitute.org/) and Integrative

128   Japanese Genome Variation Database (3.5KJPN; https://ijgvd.megabank.tohoku.ac.jp/).

129   In addition, a rare heterozygous missense variant in the *FLNB* gene (chr3:58 121

130   852C>G [GRCh37/hg19]; c.4818C>G [NM_001457.3], p.Ile1606Met [NP_001448.2]

131   [rs774972522]) was identified in the patient and the mother. The father had no

132   deleterious variants in *FLNB*. The minor allele frequency of the c.4818C>G in *FLNB*

133   variant in the general population was reported to be 0.27% in the 3.5 KJPN database. *In*

134   *silico* analyses performed using PolyPhen-2 (http://genetics.bwh.harvard.edu/pph2/) and

135   MutationTaster (http://www.mutationtaster.org) predicted that this rare variant would be

136   pathogenic. The expression analyses of the proband revealed a biallelic expression of

137   *FLNB* without abnormal splicing variants or exonic deletions (data not shown).

138   There were no mutations in *MYH3*, *RFLNB,* or other genes known to be related to

139   vertebral segmentation formation [12].

140

141   **Discussion**

142   We identified a rare maternally derived missense *FLNB* variant (c.4818C>G,

143   p.Ile1606Met) in the present patient with a typical phenotype of SCT. While SCT is

144   caused by biallelic truncating mutations in *FLNB* [1, 2, 4], the expression analyses in

145   this study showed a biallelic expression of *FLNB,* including normal transcripts of *FLNB*

146   that originated from the paternal allele in the patient, indicating that the patient is

147   certainly heterozygous for the *FLNB* variant. Furthermore, the *FLNB* variant has been

148   identified among the general Japanese population. In addition, the mother with the same

149   variant does not show the typical SCT phenotype. Collectively, the present data argue

150   against any pathological role of the missense variant in the development of SCT,

151   although the possibility that the variant might function as a susceptibility factor for the

152   development of SCT or short stature remains tenable. Thus, a mutation(s) in a new,

153   undiscovered gene(s) may be responsible for SCT in the patient.

154   In this regard, we identified a novel homozygous frameshift mutation in *RFLNA*

155   in the patient, and propose the homozygous mutation of *RFLNA* as another genetic

156   cause of SCT, based on the following findings. First, although mice with the single

157   knockout of either *Rflna* or *Rflnb* (also known as *Cfm2* and *Cfm1*, respectively)

158   displayed wild-type phenotypes, double knockout mice manifested progressive

159   scoliosis, kyphosis, vertebral fusions, intervertebral disc defects, and growth retardation

160   [13]. The above phenotype is similar to that of *Flnb*-deficient mice and of human SCT

161   patients, indicating that defects of RFLN families may lead to the phenotype of SCT in

162   humans [1, 2, 4]. At this point, there is a phenotypic difference between *Rflna* single

163   knockout mice and our patient with a homozygous *RFLNA* mutation. This may be

164   associated with the difference of their genetic background and/or gene expression

165   pattern [14]. Second, only a few heterozygous truncating variants and no homozygous

166   null variants in *RFLNA* have been registered in ExAC database, implying that biallelic

167   *RFLNA* mutations result in some pathogenic effects in humans. Third, *Rflna* is

168   expressed in the vertebral primordia, vertebral bodies and carpal bones in embryonic

169   mice and the expression is increased in prehypertrophic chondrocytes, implying the

170   positive role of RFLNA in vertebral and carpal/tarsal bone development [15]. Fourth, a

171   significantly decreased expression level of *RFLNA* has been observed in primary

172   osteoblasts derived from the spinal vertebrae in patients with adolescent idiopathic

173   scoliosis [16]. This result indicates that RFLNA has an important role in the normal

174   development and growth of the vertebral column. Finally, the variant is predicted to

175   retain the filamin binding domains (FBDs) 1 and 2 but lose FBD3 and FBD4 (Fig. 3c)

176   and thereby hardly form parallel actin bundles. Indeed, primary rib chondrocytes from

177   *Rflna* and *Rflnb* double knockout mice formed fewer actin bundles [13]. A biallelic *Flnb*

178   defect is also predicted to affect the parallel actin bundle formation. In addition, *MYH3*

179   mutations have been reported to alter TGF-β canonical signaling [3]. Thus, a defect in

180   forming actin bundles and perinuclear actin caps may be a critical mechanism

181   responsible for the development of SCT.

182   In conclusion, we propose, for the first time, an association between a

183   homozygous mutation of *RFLNA* and SCT. Further studies and the accumulation of

184   additional cases with *RFLNA* mutations are needed to clarify the pathogenic

185   significance of *RFLNA* mutations.

186

187   **Conflicts of interest**

188   The authors declare no conflicts of interest in association with the present study.

189

References

1. Krakow D, Robertson SP, King LM, Morgan T, Sebald ET, Bertolotto C, et al. Mutations in the gene encoding filamin B disrupt vertebral segmentation, joint formation and skeletogenesis. Nat Genet. 2004;36:405–10.

2. Farrington-Rock C, Kirilova V, Dillard-Telm L, Borowsky AD, Chalk S, Rock MJ, et al. Disruption of the Flnb gene in mice phenocopies the human disease spondylocarpotarsal synostosis syndrome. Hum Mol Genet. 2009;17:631–41.

3. Zieba J, Zhang W, Chong JX, Forlenza KN, Martin JH, Heard K, et al. A postnatal role for embryonic myosin revealed by MYH3 mutations that alter TGFβ signaling and cause autosomal dominant spondylocarpotarsal synostosis. Sci Rep. 2017;7:41803.

4. Xu Q, Wu N, Cui L, Wu Z, Qiu G. Filamin B: The next hotspot in skeletal research? J Genet Genomics. 2017;44:335–42

5. Salian S, Shukla A, Shah H, Bhat SN, Bhat VR, Nampoothiri S. et al. Seven additional families with spondylocarpotarsal synostosis syndrome with novel biallelic deleterious variants in FLNB. Clin Genet. 2018;94:159-64

6. Baudier J, Jenkins ZA, Robertson SP. The filamin-B-refilin axis - spatiotemporal regulators of the actin-cytoskeleton in development and disease. J Cell Sci. 2018;13:131.

7. Khatau SB, Hale CM, Stewart-Hutchinson PJ, Patel MS, Stewart CL, Searson PC, et

217   al. A perinuclear actin cap regulates nuclear shape. Proc Natl Acad Sci U S A.

218   2009;10:19017-22.

219   8. McKenna A, Hanna M, Banks E, Sivachenko A, Cibulskis K, Kernytsky A. et al. The

220   Genome Analysis Toolkit: a MapReduce framework for analyzing next-generation

221   DNA sequencing data. Genome Res. 2010;20:1297–303.

222   9. Mishima H, Sasaki K, Tanaka M, Tatebe O, Yoshiura K. Agile parallel bioinformatics

223   workflow management using Pwrake. BMC Res Notes. 2011;4:331–8.

224   10. Wang K, Li M, Hakonarson H. ANNOVAR: functional annotation of genetic variants

225   from high-throughput sequencing data. Nucleic Acids Res. 2010;38:e164.

226   11. Morimoto Y, Shimada-Sugimoto M, Otowa T, Yoshida S, Kinoshita A, Mishima H,

227   et al. Whole-exome sequencing and gene-based rare variant association tests suggest

228   that PLA2G4E might be a risk gene for panic disorder. Transl Psychiatry. 2018;8:41

229   12. Gibb S, Maroto M, Dale JK. The segmentation clock mechanism moves up a notch.

230   Trends Cell Biol. 2010;20:593–600.

231   13. Mizuhashi K, Kanamoto T, Moriishi T, Muranishi Y, Miyazaki T, Terada K, et al.

232   Filamin-interacting proteins, Cfm1 and Cfm2, are essential for the formation of

233   cartilaginous skeletal elements. Hum Mol Genet. 2014;23:2953–67.

234   14. Liao BY, Zhang J. Null mutations in human and mouse orthologs frequently result in

235   different phenotypes. Proc Natl Acad Sci U S A. 2008:105:6987–92.

236   15. Gay O, Gilquin B, Nakamura F, Jenkins ZA, McCartney R, Krakow D, et al. RefilinB

237   (FAM101B) targets filamin A to organize perinuclear actin networks and regulates

238   nuclear shape. Proc Natl Acad Sci U S A. 2011;12:11464–9.

239   16. Fendri K, Patten SA, Kaufman GN, Zaouter C, Parent S, Grimard G, et al. Microarray

240   expression profiling identifies genes with altered expression in Adolescent Idiopathic

241   Scoliosis. Eur Spine J. 2013;22:1300–11.

242

243 **Titles and legends to figures**

244 **Fig. 1. A schematic illustration of filamins and the formation of parallel actin**

245 **bundles and perinuclear actin caps.**

246 (a) The structure of a monomeric chain of filamins. Filamin contains two calponin

247 homology domains (CH1 and CH2) that have actin binding affinity followed by 24 β-

248 pleated sheet immunoglobulin (Ig)-like repeats (ellipses). The repeats are interrupted by

249 two flexible hinge regions (H1 and H2) that allow filamins for structural flexibility. The

250 Ig-like repeats contain another actin-binding domain (ABD), two RFLNs binding

251 domains, and a C-terminal domain that contains a mechanosensor region (MSR) [5].

252 (b) Schematic illustration of a vertebrate filamin dimer (left) and formation of parallel

253 actin bundles (right). Under the TGF-β stimulations, filamins bind to RFLNs and

254 transform their connecting actin into a parallel bundle structure. During this process,

255 MSRs release their holding mediators like SMADs to induce downstream signals.

256 (c) The parallel actin bundles accumulate and produce perinuclear actin caps. These

257 actin dynamics are necessary for cellular migration and differentiation. These figures

258 are modified from those of Baudier et al [6] and Khatau et al [7].

259 **Fig. 2. Radiological examinations of the patient.**

260 (a) Dorsal (left, middle) and ventral (right) views of spinal three-dimensional computed

261 tomography at 1 year 7 months of age show scoliosis, vertebral fusions and dysraphisms

262 (white arrows). (b) Carpal (left) and tarsal (right) synostoses at 1 year 2 months of age

263 (white arrows).

264 **Fig. 3. The *RFLNA* variant of the proband.**

265 (a) Electrochromatograms delineating a homozygous frameshift *RFLNA* variant

266   (c.241delC, p.(Leu81Cysfs*111)) (NM_181709, NP_859060.3) in the proband. (b)

267   PCR-based expression analyses for *RFLNA* (35 cycles) (upper) and the sequencing

268   analysis (lower). *PGK1* has been used as an internal control (20 cycles). The mutant

269   *RFLNA* is expressed in lymphoblastoid cell lines derived from the proband as well as

270   the parents with the heterozygous *RFLNA* mutation. NC, negative control. (c) The

271   position of the *RFLNA* variant and the estimated structure of the mutant protein. This

272   variant is predicted to skip the initial termination, and result in the production of an

273   additional 110 aberrant amino acids (a gray box). This mutated protein is predicted to

274   retain the filamin binding domains (FBDs) 1 and 2 but lose the FBD3 and FBD4 (blue
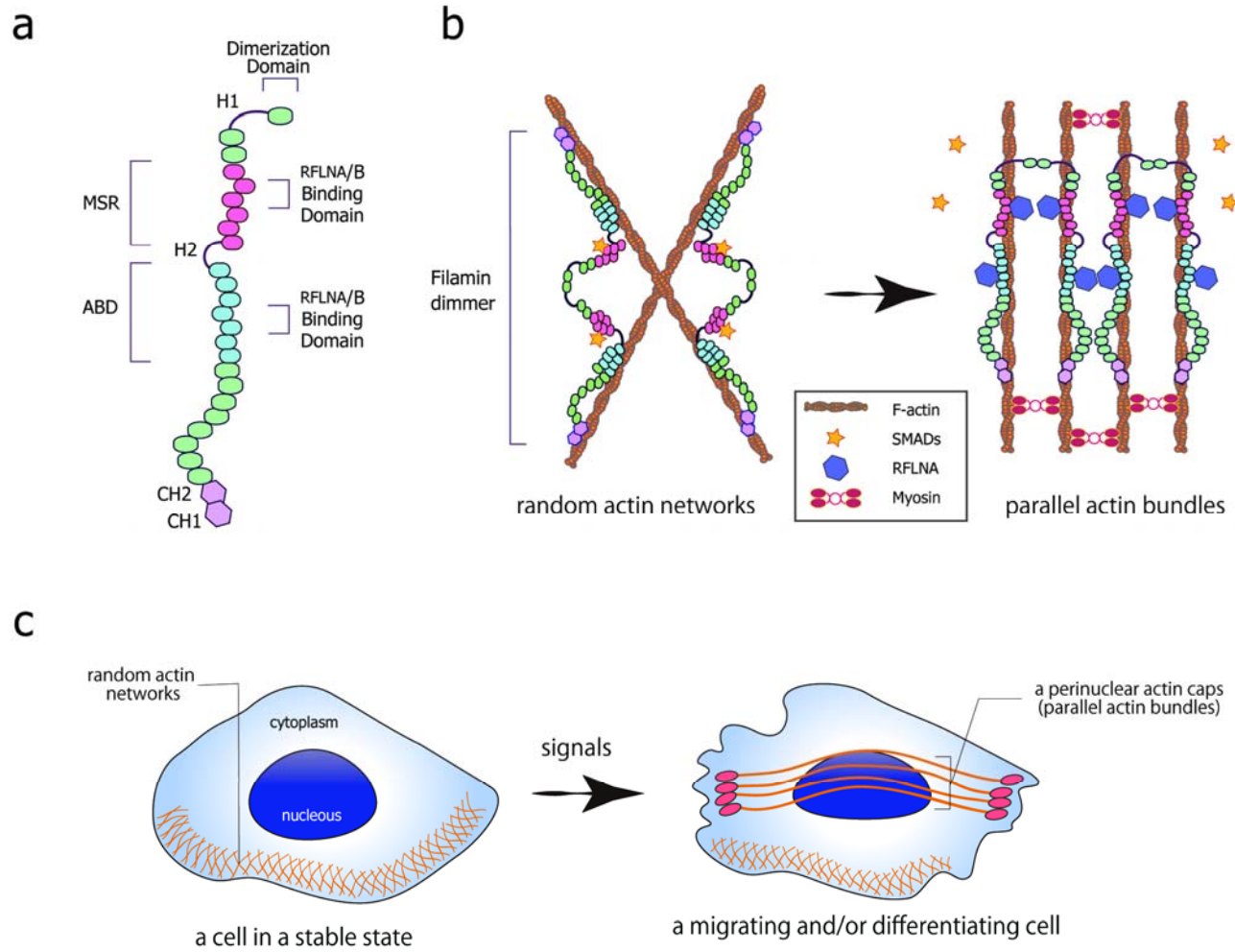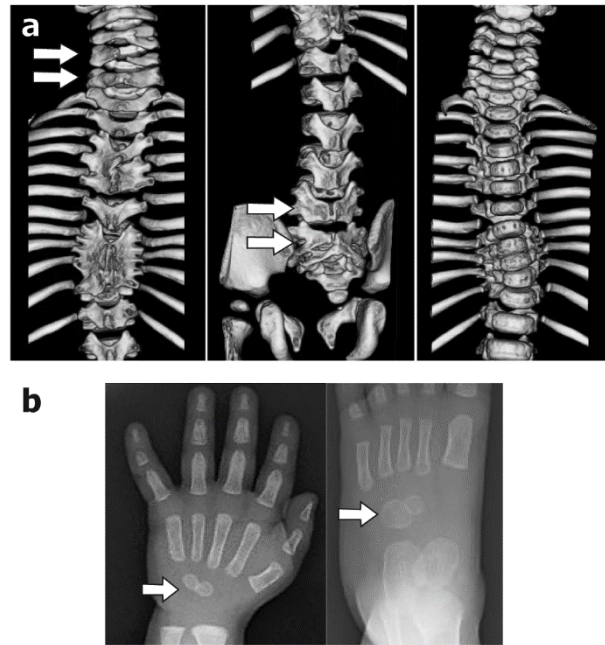
275   boxes).

Fig. 1

Fig. 2

Fig. 3